



# Retrosynthetic Analysis Applied to Clip-off Chemistry: Synthesis of Four Rh(II)-Based Complexes as Proof-of-Concept

Anna Broto-Ribas<sup>+</sup>, Sara Ruiz-Relaño<sup>+</sup>, Jorge Albalad,<sup>\*</sup> Yunhui Yang, Felipe Gándara, Judith Juanhuix, Inhar Imaz,<sup>\*</sup> and Daniel Maspoch<sup>\*</sup>

**Abstract:** Clip-off Chemistry is a synthetic strategy that our group previously developed to obtain new molecules and materials through selective cleavage of bonds. Herein, we report recent work to expand Clip-off Chemistry by introducing into it a retrosynthetic analysis step that, based on virtual extension of the products through cleavable bonds, enables one to define the required precursor materials. As proof-of-concept, we have validated our new approach by synthesising and characterising four aldehyde-functionalised Rh(II)-based complexes: a homoleptic cluster; a *cis*-disubstituted paddlewheel cluster; a macrocycle; and a crown.

## Introduction

New molecules and materials are and will be key for our society, so that their design and synthesis will still be a

vibrant challenge for chemists.<sup>[1–3]</sup> Traditionally, the way that chemists envision their synthesis is ultimately driven by bond formation steps (i.e. from simple starting materials to a complex product)<sup>[4–7]</sup> or, to a lesser extent, by bond-breaking.<sup>[8,9]</sup> We have recently developed an alternative synthetic approach, named Clip-off Chemistry, which proposes using bond breaking as the core synthetic step.<sup>[10]</sup> Clip-off Chemistry benefits from the rich repertoire of molecules and materials synthesised by traditional methods by using these as precursors that, once conferred with cleavable sites, can generate new molecules and materials upon selective bond cleavage.

In a first attempt to demonstrate the feasibility of Clip-off Chemistry, we have recently applied this concept using reticular materials as the starting precursors. We reasoned that reticular materials such as metal–organic frameworks (MOFs)<sup>[11]</sup> and metal-organic polyhedra (MOPs)<sup>[12,13]</sup> would be ideal candidates for the following three reasons. Firstly, they are all formed by periodic structures, such that their constituent organic linkers are perfectly ordered.<sup>[14,15]</sup> Secondly, they are porous, so reagents can diffuse throughout their structures to reach all cleavable sites.<sup>[16–18]</sup> Finally, Reticular Chemistry dictates that for a given structure, the constituents can be chemically functionalised pre- and/or post-synthetically, without any loss in structural connectivity.<sup>[19–21]</sup> This idea translates to the ability to encode the organic linkers of an existing reticular material with synthetic information by inserting into them cleavable groups without altering the linkers' shape or directionality, to ultimately enable the synthesis of analogous cleavable isorecticular structures.<sup>[22]</sup> In our first report, we inserted olefinic groups as cleavable bonds in MOFs/MOPs, and then selectively and quantitatively cleaved those bonds by ozonolysis. Thus, we demonstrated Clip-off Chemistry by synthesising two topologically distinct 3D MOFs (each from a distinct MOF precursor) and one metal-organic macrocycle (from a single precursor MOP).<sup>[10]</sup>

Herein, we advance on the development of Clip-off Chemistry by introducing the concept of retrosynthetic analysis. In Organic Chemistry, retrosynthesis is a crucial process that allows defining the reactants and the chemical reactions needed to form a desired product (Figure 1a).<sup>[23–25]</sup> This process starts by virtually dissecting stepwise the product into simple and easily-accessible synthons. Each synthon is later chemically translated to suitable reagent precursors, essentially building backwards the series of chemical reactions that will be followed to synthesise the product. However, in Clip-off Chemistry, we cannot apply

[\*] A. Broto-Ribas,<sup>+</sup> S. Ruiz-Relaño,<sup>+</sup> Dr. J. Albalad, Y. Yang, Dr. I. Imaz, Prof. Dr. D. Maspoch  
Catalan Institute of Nanoscience and Nanotechnology (ICN2), CSIC and The Barcelona Institute of Science and Technology Campus UAB, Bellaterra, 08193 Barcelona (Spain)  
and  
Departament de Química, Facultat de Ciències, Universitat Autònoma de Barcelona (UAB)  
Cerdanyola del Vallès, 08193 Barcelona (Spain)  
E-mail: jorge.albalad@icn2.cat  
inhar.imaz@icn2.cat  
daniel.maspoch@icn2.cat

Dr. F. Gándara  
Materials Science Institute of Madrid (ICMM), Consejo Superior de Investigaciones Científicas (CSIC)  
Calle Sor Juana Inés de la Cruz, 3, 28049 Madrid (Spain)

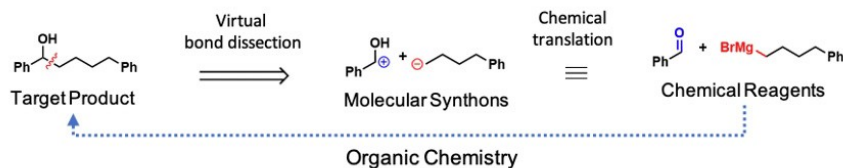
Dr. J. Juanhuix  
Alba Synchrotron Light Facility  
Cerdanyola del Vallès, 08290 Barcelona (Spain)

Prof. Dr. D. Maspoch  
ICREA  
Pg. Lluís Companys 23, 08010 Barcelona (Spain)

[†] These authors contributed equally to this work.

© 2023 The Authors. Angewandte Chemie International Edition published by Wiley-VCH GmbH. This is an open access article under the terms of the Creative Commons Attribution Non-Commercial License, which permits use, distribution and reproduction in any medium, provided the original work is properly cited and is not used for commercial purposes.

## a) Retrosynthetic analysis in Organic Chemistry



## b) Retrosynthetic analysis in Clip-off Chemistry

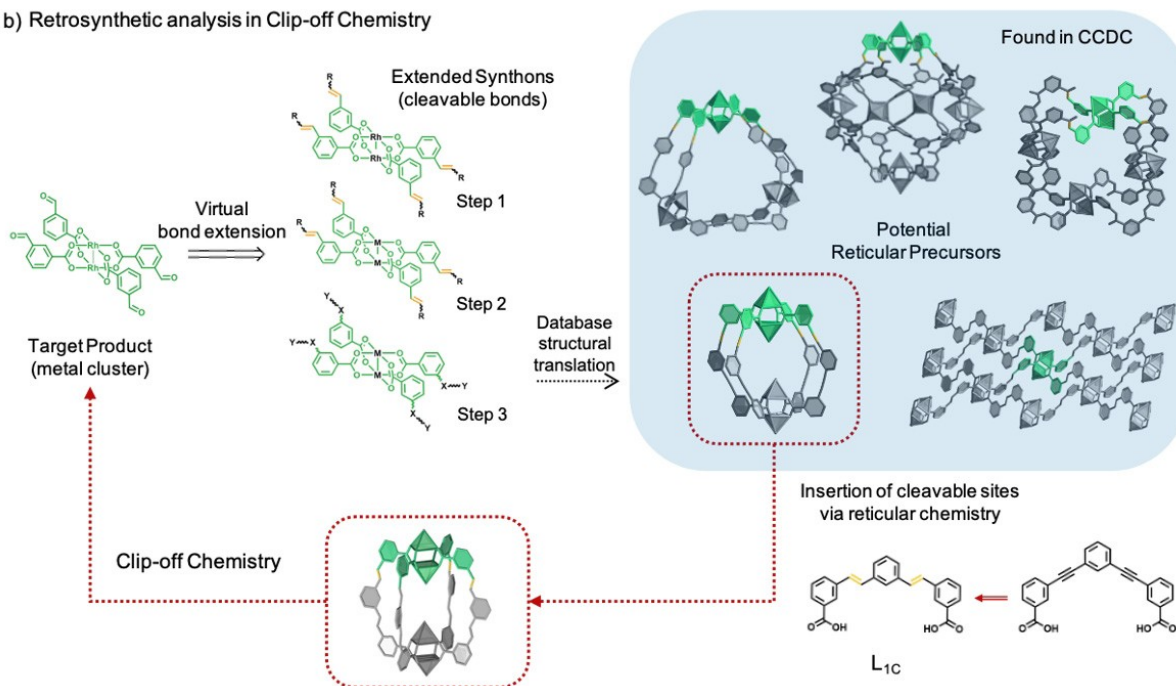


**Figure 1.** (a) Schematic example of the retrosynthetic analysis of bond formation steps in Organic Chemistry. A target bond is virtually dissected into molecular synthons, which later get chemically translated into logical reagent substrates. (b) Schematic of retrosynthetic analysis in Clip-off Chemistry, used here to obtain the product  $[Rh_2(3FBA)_4]$ . In it, the final product is virtually extended via cleavable bonds into a logical structure (discrete or periodic), which later is structurally translated into suitable reported lattices from several structural databases. If required, a final step consisting of isorecticular conversion of the reported linkers into an alkene-tagged analogue can be performed.

this style of retrosynthetic analysis, as it is ultimately based on bond breaking rather than bond formation steps. In fact, we should conceive it in an opposite way: retrosynthesis in Clip-off Chemistry should start by virtually connecting the target product through cleavable bonds into an initial molecule or material, which will be used as the sacrificial precursor to synthesise our target product via bond breaking reactions (Figure 1b).

As proof-of-concept, we employed our retrosynthetic approach to design and synthesise four novel, aldehyde-functionalised, Rh(II) metal-organic materials: a homoleptic paddlewheel cluster; a *cis*-disubstituted paddlewheel cluster; a triangular macrocycle; and a crown-like architecture. In each case, we followed a three-step process: firstly, retrosynthetic conversion of the target product into a suitable reticular precursor that contains olefinic bonds as future cleavage sites; secondly, synthesis of that precursor; and finally, cleavage of the olefinic bonds (by ozonolysis). We characterised all four products through a battery of

analytical techniques and single-crystal X-ray diffraction (SCXRD).

## Results and Discussion

We began with the synthesis of a homoleptic Rh–Rh paddlewheel cluster, as the simplest test-case scenario. As ozonolysis enables transformation of an olefinic bond into either an aldehyde (under reductive conditions) or a carboxylic acid (under oxidative conditions),<sup>[26]</sup> we envisaged this cluster to be built up with four 3-formylbenzoate (3FBA) ligands under strict control of the reaction conditions (Figure 1b). Thus, our initial target product was a Rh–Rh paddlewheel cluster of formula  $[Rh_2(3FBA)_4]$ , which is functionalised with four aldehyde groups located at the *meta* position of each phenyl ring. Once we had defined the product, we conducted the retrosynthetic analysis by the conceptual assembly of this cluster through cleavable

olefinic bonds (Figure 1b, extended synthon) into a suitable reticular material.

To facilitate identification of the desired reticular material, we searched the Cambridge Crystallographic Data Centre (CCDC) database (ConQuest v. 2022.3.0, CCDC, Cambridge, UK)<sup>[27]</sup> for structures that would contain such an extended synthon. To this end, we followed a stepwise search protocol that can be applied to retrosynthetic analysis of any metal-organic product in Clip-off Chemistry. In Step 1, one searches for structures containing the exact extended synthon (in our case, the synthon comprising a Rh(II) paddlewheel cluster extended via olefinic cleavable bonds). If that is unsuccessful, then one proceeds to Step 2: expanding the search to encompass analogous synthons made with any metal ion. Finally, if that also fails, the one can do Step 3: an even broader search, of structures containing a simplified synthon (in our case, a paddlewheel cluster of any metal, extended via any organic atom). Note here that Steps 2 and 3 involve the use of isorecticular chemistry to synthesise the suitable precursor material, converting the linkers of any successful search into alkene-based analogues, and/or substituting the identified metal ions with the desired ones. In our search for  $[\text{Rh}_2(3\text{FBA})_4]$ , steps 1 and 2 failed. However, in Step 3, we found five suitable structures (Figure 1b): one Cu(II)-based double-wall triangular macrocycle;<sup>[28]</sup> one Cu(II)-based octahedral MOP;<sup>[29]</sup> one Cu(II)-based square-like MOP;<sup>[30]</sup> several lantern-type MOPs made of different metal ions [including Rh(II)];<sup>[31]</sup> and one extended two-dimensional Cu(II)-based MOF.<sup>[32]</sup> Among these structures, we selected the lantern-type MOP as our candidate precursor, as it was both the simplest and the only one containing Rh(II) ions. This inspired us to design a similar lantern-type MOP embedded with alkene bonds, by substituting the reported 3,3'-phenylenebis(ethyne-2,1-diyl)dibenzoic acid linker with one containing olefinic bonds, the (*E*)-3,3'-(1,3-phenylenebis(ethene-2,1-diyl))dibenzoic acid linker ( $\text{L}_{1\text{C}}$ ; Figure 1b). The precursor lantern-type MOP of formula  $[\text{Rh}_2(\text{L}_{1\text{C}})_2]_2$  was obtained by solvothermal synthesis in *N,N*-dimethylacetamide (DMA) at 100 °C. The formation of this MOP was confirmed by MALDI-ToF spectrometry (experimental  $[m/z] = 1884.9$ ; simulated  $[m/z]$  for  $[\text{Rh}_4(\text{L}_{1\text{C}})_4 + \text{H}^+]^+ = 1886.2$ ) and  $^1\text{H}$  NMR spectroscopy (Figures S5–S6, ESI†). Crystallisation of the green powder by vapour diffusion of diethyl ether into a DMA solution containing 4-*tert*-butylpyridine yielded parallelepiped-shaped purple crystals from which SCXRD analysis revealed the expected lantern-type structure (Figure 2a, left).

With the precursor in hand, we carried out the ozonolysis in a DMA/DMSO (1:0.7 v/v) mixture under a flow of ozone (10.4 mmol/h) at 0 °C for 15 minutes in the presence of dimethyl sulphide (DMS, 0.3 mL) as reducing agent. The DMSO was required to protect the axial Rh(II) metal sites from ozone by coordination. The products were precipitated out and filtered off and crystallised from acetone/water by slow evaporation (see ESI for details). Encouragingly, SCXRD of the resulting crystals confirmed the formation of the expected  $[\text{Rh}_2(3\text{FBA})_4]$  cluster (Figure 2a, right), with a yield of 96 %. Mass spectrometric

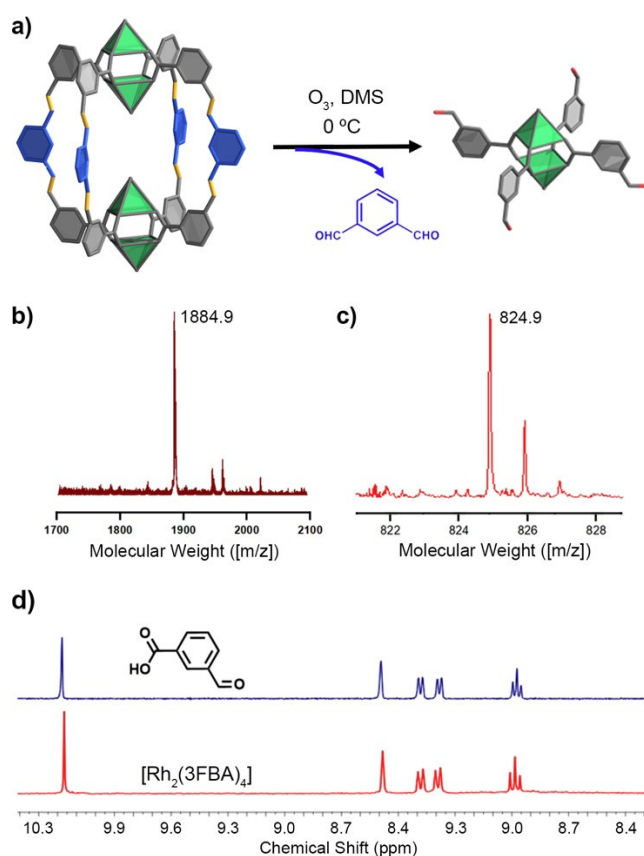


**Figure 2.** (a) Schematic of the Clip-off synthesis of the homoleptic paddlewheel  $[\text{Rh}_2(3\text{FBA})_4]$  cluster from  $[\text{Rh}_2(\text{L}_{1\text{C}})_2]_2$ . Representations of  $[\text{Rh}_2(\text{L}_{1\text{C}})_2]_2$  (left) and  $[\text{Rh}_2(3\text{FBA})_4]$  (right) corresponding to their X-ray crystal structures. Axial capping agents (pyridine derivatives, solvents) and H atoms were omitted for clarity. (b) MALDI-ToF spectrum of  $[\text{Rh}_2(\text{L}_{1\text{C}})_2]_2$ . (c) ESI-MS spectrum of  $[\text{Rh}_2(3\text{FBA})_4]$ . (d) Digested  $^1\text{H}$  NMR spectra of  $[\text{Rh}_2(3\text{FBA})_4]$  (red) and its molecular component, 3FBA (blue).

analysis confirmed the formation of the product, with an experimental molecular weight of  $[m/z] = 824.9$  (simulated  $[m/z]$  for  $[\text{Rh}_2(3\text{FBA})_4 + \text{Na}^+]^+ = 824.9$ , Figure S7).  $^1\text{H}$  NMR analysis of the digested precipitate showed a quantitative loss of the starting  $\text{L}_{1\text{C}}$  signals in  $[\text{Rh}_2(\text{L}_{1\text{C}})_2]_2$  ( $\text{HC}=\text{CH} \delta \approx 7.4$  ppm, Figure S11), as well as a proportional formation of new signals perfectly matching those expected for 3FBA ( $\text{CHO} \delta = 10.2$  ppm, Figure 2d). Concurrently,  $^1\text{H}$  NMR analysis of the acidic supernatant from the ozonolysis reaction revealed 1,3-benzenedicarboxaldehyde as the only side-product (Figure S11).

Having demonstrated the feasibility of retrosynthetically designing reticular precursors by connecting the products through cleavable bonds, we decided to extend our approach to the synthesis of a product that we expected to be more difficult to obtain using traditional synthetic methods. Thus, our second target was the *cis*-geometric isomer of the Rh–Rh paddlewheel cluster coordinated by two 3FBA ligands and two 4FBA (where 4FBA is 4-formylbenzoate) ligands. This new cluster, of formula  $[\text{Rh}_2(3\text{FBA})_2(4\text{FBA})_2]$ , is functionalised with two aldehyde groups at the *meta*



position and two at the *para* position of the phenyl rings, as shown in Figure 3a. Indeed, such a product is quite challenging to obtain through bottom-up assembly, as it would likely produce a statistical combination of homoleptic and mixed-linker Rh-paddlewheel clusters, whether mono-, di-, or tri-substituted.<sup>[33,34]</sup> Furthermore, *trans* clusters are far more common in the literature than *cis* clusters, further increasing the complexity of obtaining our target product by traditional methods.<sup>[35,36]</sup> Thus, we challenged our Clip-off Chemistry for the synthesis of this new *cis*-[Rh<sub>2</sub>(3FBA)<sub>2</sub>(4FBA)<sub>2</sub>] cluster in high yields and phase purity. Analysis of the target product shows that the starting precursor must contain at least two distinct cleavable linkers, with alkene groups in the *meta* positions and *para* positions, respectively, relative to the carboxylate sites. Additionally, both linkers must be connected to Rh–Rh nodes in a *cis* conformation (Figure 3a). After searching for suitable candidates, we found the perfect precursor in a family of heteroleptic MOPs (Figure 3a).<sup>[37–39]</sup> These heteroleptic MOPs are built from two different linker groups, distributed regularly into axial and equatorial positions around 6 paddlewheel nodes. Closer analysis of their structure revealed that the linkers are homogeneously distributed as two pairs of *cis*-distributed bridges in between clusters, thereby making them perfect candidates for our *cis*-cluster synthesis. Therefore, we

reasoned that if we could design suitable cleavable linkers for each position (i.e. equatorial and axial), we would be able to obtain our target product via Clip-off Chemistry. After virtually extending the product, we decided to employ the linkers (*E*)-3,3'-stilbenedicarboxylic acid (L<sub>2C</sub>) and (*E*)-4,4'-(1,3-phenylene-bis(ethene-2,1-diyl))dibenzoic acid (L<sub>3C</sub>) as the best candidates to generate the moieties 3FBA and 4FBA, respectively, through ozonolysis (Figure 3a).

We synthesised the MOP of formula [Rh<sub>2</sub>(L<sub>2C</sub>)(L<sub>3C</sub>)<sub>6</sub>] through a solvothermal reaction of L<sub>2C</sub>, L<sub>3C</sub> and rhodium acetate. Unfortunately, our attempts to obtain single crystals suitable for SCXRD were unsuccessful. Nonetheless, we were able to characterise the digested solid by <sup>1</sup>H NMR spectroscopy, which confirmed the formation of a single entity comprising a 1:1 linker ratio (Figure S12). We confirmed the formation of [Rh<sub>2</sub>(L<sub>2C</sub>)(L<sub>3C</sub>)<sub>6</sub>] by MALDI-ToF spectrometry: the spectrum contained a broad peak centred at  $[m/z] = 5530.3$ , which agrees with the expected mass of  $[m/z] = 5524.6$  for the targeted formula [Rh<sub>12</sub>(L<sub>2C</sub>)<sub>6</sub>(L<sub>3C</sub>)<sub>6</sub> + H<sup>+</sup> · 6 DMSO (Figure S13). Ozonolysis of [Rh<sub>2</sub>(L<sub>2C</sub>)(L<sub>3C</sub>)<sub>6</sub>] in DMA/DMSO/DMS mixture (1:0.7:0.3 v/v/v) under the same conditions at 0 °C for 15 minutes resulted in quantitative alkene bond cleavage, and [Rh<sub>2</sub>(3FBA)<sub>2</sub>(4FBA)<sub>2</sub>] was obtained in 92 % yield. Slow evaporation of a solution of the product in a mixture of MeCN/H<sub>2</sub>O (1:1 v/v)

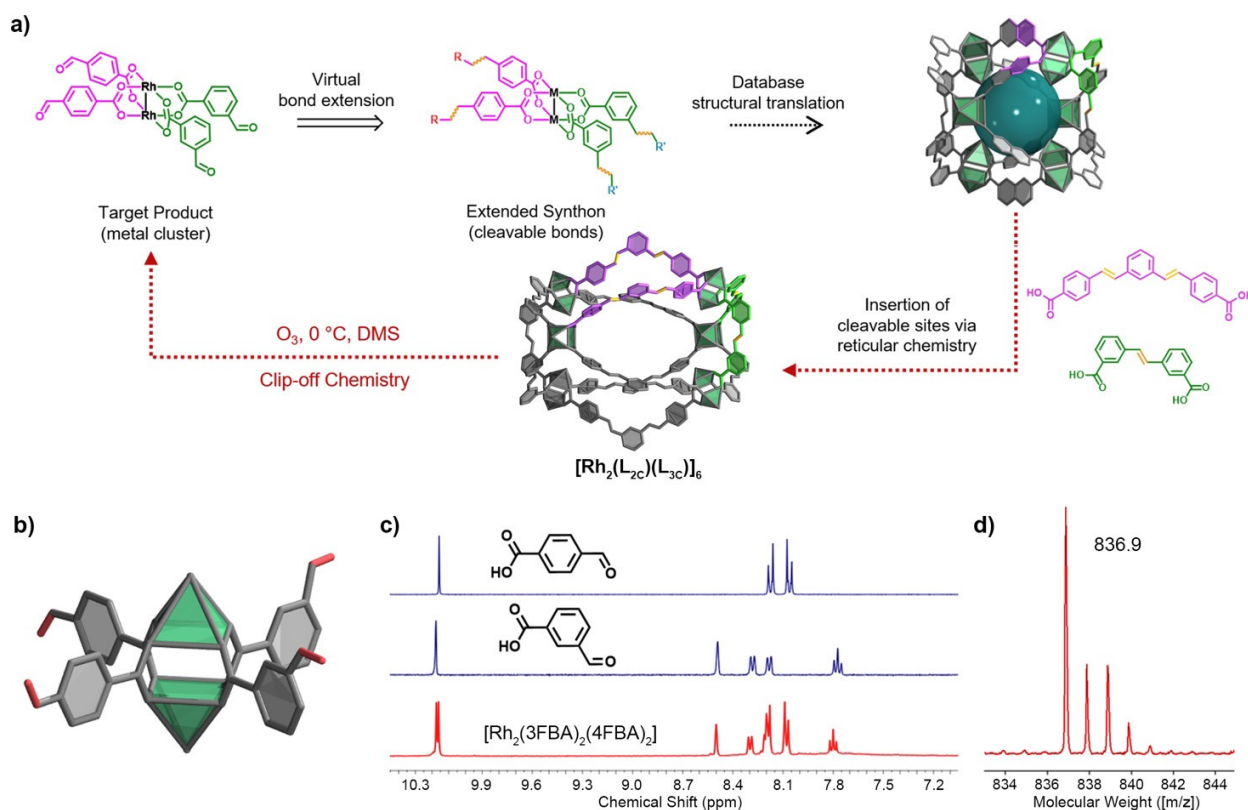


**Figure 3.** (a) Schematic representation of the retrosynthetic analysis conducted for the synthesis of the *cis*-disubstituted [Rh<sub>2</sub>(3FBA)<sub>2</sub>(4FBA)<sub>2</sub>] cluster via Clip-off Chemistry, from which the precursor [Rh<sub>2</sub>(L<sub>2C</sub>)(L<sub>3C</sub>)<sub>6</sub>] was identified. (b) Single-crystal structure of [Rh<sub>2</sub>(3FBA)<sub>2</sub>(4FBA)<sub>2</sub>]. (c) Digested <sup>1</sup>H NMR spectra of [Rh<sub>2</sub>(3FBA)<sub>2</sub>(4FBA)<sub>2</sub>] (red) versus those of its molecular components: 3FBA and 4FBA (blue). (d) ESI-MS spectrum of [Rh<sub>2</sub>(3FBA)<sub>2</sub>(4FBA)<sub>2</sub>].

afforded plate-shaped crystals suitable for SCXRD (Figure 3b). Synchrotron diffraction data confirmed the integrity of Rh–Rh paddlewheel clusters after ozonolysis, and the quantitative cleavage of both linkers into the expected product. SCXRD data revealed an experimental 50:50 occupancy distribution between the 3- and 4-substituted FBA ligands, corresponding to an overlay of an average of superimposed *cis*-clusters in different orientations (Figure S14). NMR analysis of the digested product revealed a 1:1 ratio of 3FBA and 4FBA ligands (Figures 3c, S15). Likewise, ESI-MS analysis of the products showed a single entity with the expected molecular weight attributed to  $[\text{Rh}_2(3\text{FBA})_2(4\text{FBA})_2]$  (experimental  $[m/z] = 836.9$ , simulated  $[m/z]$  for  $[[\text{Rh}_2(3\text{FBA})_2(4\text{FBA})_2] + \text{Cl}^-] = 836.9$ ; Figures 3d, S16). Analysis of the acid supernatant used to precipitate the product did not reveal any residual traces of free rhodium ions, thereby confirming the inert character of the metal cluster upon ozone exposure (Table S5). Additionally,  $^1\text{H}$  NMR analysis of the supernatant showed exclusively the presence of 1,3-diformylbenzene (side product expected from the reductive ozonolysis of  $\text{L}_{3\text{C}}$ ), thus ruling out any potential linker exchange/substitution around the Rh–Rh node (Figure S19).

Reflecting on the aforementioned heteroleptic MOP precursor, which contains two different linkers, we envisioned that in such MOPs, we could mix cleavable linkers with inert ones. We reasoned that this combination could follow either of two distinct routes. In the first one, the inert linker would occupy the equatorial positions, such that clipping of the precursor should generate a crown-shaped product (Figure 4a). In the second case, the axial sites would be resistant to ozone and therefore, clipping should generate a macrocyclic product (Figure 5a). In both cases, we restricted our search for the suitable precursors to those reported in this family of heteroleptic MOPs, from which we identified two previously reported MOPs:  $[\text{Rh}_2(\text{L}_{2\text{C}})(\text{NDC})_6]$  (where  $\text{NDC} = 2,7\text{-naphthalenedicarboxylic acid}$ ), to provide the *crown*; and  $[\text{Rh}_2(t\text{BuBDC})(\text{L}_{2\text{C}})]_6$  (where  $t\text{BuBDC} = 5\text{-tert-butylisophthalic acid}$ ), to give the *macrocycle*.

We synthesised the first heteroleptic MOP precursor with inert equatorial positions from a mixture of  $\text{L}_{2\text{C}}$  and NDC. SCXRD analysis and spectroscopic characterisation of the product confirmed the formation of the targeted heteroleptic cage of formula  $[\text{Rh}_2(\text{L}_{2\text{C}})(\text{NDC})_6]$ , with six cleavable axial  $\text{L}_{2\text{C}}$  linkers and six inert equatorial NDC moieties (Figure 4a, Figures S20–S21).  $[\text{Rh}_2(\text{L}_{2\text{C}})(\text{NDC})_6]$  was treated with ozone for 20 minutes under the standard reductive conditions. The product was collected by filtration after precipitation, washed with water, and obtained in 70 % yield after crystallisation via ether vapour diffusion to a THF solution containing 4-*tert*-butylpyridine. The resultant crystals were characterised by SCXRD, using synchrotron diffraction data that was collected at a maximum resolution of 1.3 Å, suggesting the synthesis of the  $[\text{Rh}_2(3\text{FBA})_2(\text{NDC})_6]$  crown (Figure 4a). The formation and phase purity of the targeted  $[\text{Rh}_2(3\text{FBA})_2(\text{NDC})_6]$  crown functionalised with aldehyde groups was further confirmed by spectroscopic analysis, revealing the lack of all the characteristic peaks of  $\text{L}_{2\text{C}}$  (olefinic protons at  $\delta = 7.45$  ppm; and aromatic

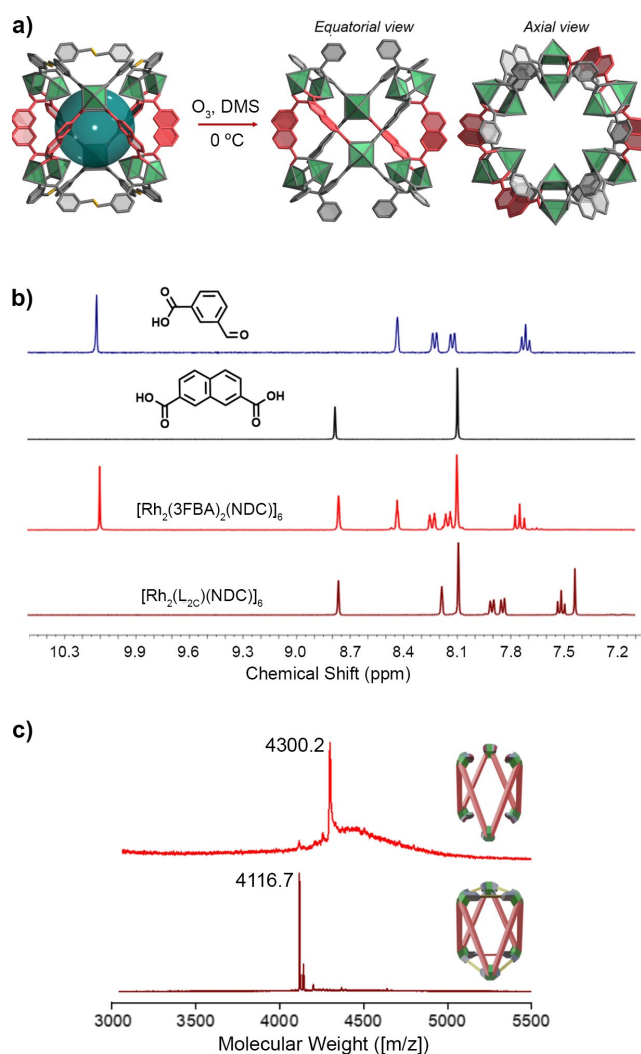


**Figure 4.** (a) Schematic of the Clip-off Chemistry synthesis of the crown-shaped  $[\text{Rh}_2(3\text{FBA})_2(\text{NDC})_6]$  complex, using the  $[\text{Rh}_2(\text{L}_{2\text{C}})(\text{NDC})_6]$  MOP as precursor. Representations of  $[\text{Rh}_2(\text{L}_{2\text{C}})(\text{NDC})_6]$  (left) and  $[\text{Rh}_2(3\text{FBA})_2(\text{NDC})_6]$  (right) correspond to their X-ray crystal structures. (b) Digested  $^1\text{H}$  NMR spectra of the  $[\text{Rh}_2(\text{L}_{2\text{C}})(\text{NDC})_6]$  precursor (dark red) and the crown (red), versus those of their molecular components: NDC (black) and 3FBA (blue). (c) MALDI-ToF spectra of the  $[\text{Rh}_2(\text{L}_{2\text{C}})(\text{NDC})_6]$  precursor (dark red) and the synthesised crown (red).

protons at  $\delta = 8.19$  ppm, 7.92 ppm, 7.85 ppm and 7.52 ppm) by digestion  $^1\text{H}$  NMR (Figure 4b). Instead, the  $^1\text{H}$  NMR spectrum revealed the characteristic signals of NDC (phenyl protons at  $\delta = 8.74$  ppm and 8.08 ppm) and those of 3FBA (aldehyde proton at  $\delta = 10.07$  ppm; phenyl protons at  $\delta = 8.41$  ppm, 8.21 ppm, 8.13 ppm and 7.73 ppm). Moreover, the integrated spectrum indicated a 3FBA/NDC acid-proton ratio of 2:1, consistent with the formula expected for the crown (Figure S22). The formation of the Rh(II)-based crown was unambiguously corroborated by MALDI-TOF (Figure 4c), which showed the molecular weight increase expected for a product of formula  $[\text{Rh}_{12}(3\text{FBA})_{12}(\text{NDC})_6 + \text{H}^+]^+$  (experimental  $[m/z] = 4300.2$  expected  $[m/z] = 4306.8$ , Figure S23); in comparison to the  $[\text{Rh}_2(\text{L}_{2\text{C}})(\text{NDC})_6]$  precursor.

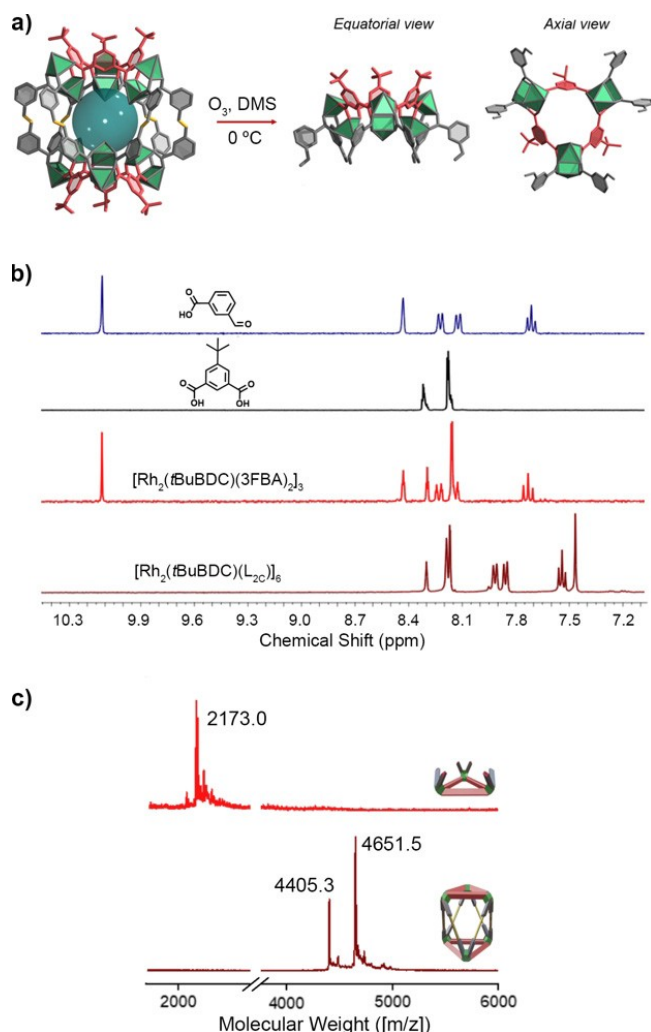


**Figure 5.** (a) Schematic of the Clip-off Chemistry synthesis of the triangular  $[\text{Rh}_2(\text{tBuBDC})(3\text{FBA})_2]_3$  macrocycle, using the MOP  $[\text{Rh}_2(\text{tBuBDC})(\text{L}_{2\text{C}})]_6$  as precursor. The representation of  $[\text{Rh}_2(\text{tBuBDC})(\text{L}_{2\text{C}})]_6$  (left) corresponds to its X-ray crystal structure, whereas those of  $[\text{Rh}_2(\text{tBuBDC})(3\text{FBA})_2]_3$  (right) are graphic models. (b) Digested  $^1\text{H}$  NMR spectra of the  $[\text{Rh}_2(\text{tBuBDC})(\text{L}_{2\text{C}})]_6$  precursor (dark red) and the macrocycle (red) versus those of their molecular components:  $\text{tBuBDC}$  (black) and  $3\text{FBA}$  (blue). (c) MALDI-ToF spectra of the  $[\text{Rh}_2(\text{tBuBDC})(\text{L}_{2\text{C}})]_6$  precursor (dark red) and the synthesised macrocycle (red).

precursor (experimental  $[m/z] = 4116.7$ ; expected for  $[\text{Rh}_{12}(\text{L}_{2\text{C}})_6(\text{NDC})_6 + \text{H}^+]^+$   $[m/z] = 4116.4$ ). Finally, analysis of the supernatant (Table S5, Figure S26) did not reveal any rhodium ions or free  $3\text{FBA}$  moieties, thus confirming the selectivity of the method.

In our final example, we synthesised a heteroleptic MOP precursor, the one exhibiting ozone-inert axial positions, using  $\text{tBuBDC}$  and  $\text{L}_{2\text{C}}$  linkers. SCXRD analysis of the product revealed a heteroleptic MOP cage of formula  $[\text{Rh}_2(\text{tBuBDC})(\text{L}_{2\text{C}})]_6$ , composed of six paddlewheel Rh–Rh SBUs connected through six axial  $\text{tBuBDC}$  linkers and six equatorial  $\text{L}_{2\text{C}}$  linkers poised for Clip-off Chemistry (Figures 5a, S27–28). Thus, a solution of  $[\text{Rh}_2(\text{tBuBDC})(\text{L}_{2\text{C}})]_6$  in DMA/DMSO/DMS (1:0.7:0.3 v/v/v) was subjected to ozo-

lysis at  $0^\circ\text{C}$  for 30 minutes under reductive conditions, which cleaved the MOP structure into two identical halves, with a yield of 65 %. Indeed, although we could not solve its crystal structure, we confirmed formation of the expected metal-organic Rh-macrocycle by comparing  $^1\text{H}$  NMR spectra of the starting  $[\text{Rh}_2(\text{tBuBDC})(\text{L}_{2\text{C}})]_6$  with that of the ozonated product (Figure 5b). The  $^1\text{H}$  NMR spectrum lacked all the characteristic peaks of  $\text{L}_{2\text{C}}$  (olefinic protons at  $\delta = 7.45$  ppm; and phenyl protons at  $\delta = 8.18$  ppm, 7.90 ppm, 7.84 ppm and 7.53 ppm). However, it revealed the characteristic signals of  $\text{tBuBDC}$  (phenyl protons at  $\delta = 8.30$  ppm and 8.16 ppm; and *tert*-butyl protons at  $\delta = 1.31$  ppm) and those of  $3\text{FBA}$  with the expected 1:2 ratio (Figure S29). This integrated spectrum indicated the quantitative transformation into a Rh-macrocycle. This was supported by MALDI-TOF analysis (Figure 5c) where the spectrum of the reaction product showed only the macrocycle  $[\text{Rh}_6(3\text{FBA})_6(\text{tBuBDC})_3 + \text{H}^+]^+$   $[m/z] = 2173.0$  (simulated  $[m/z] = 2172.9$ , Figure S30) and nothing for the  $[\text{Rh}_2(\text{tBuBDC})(\text{L}_{2\text{C}})]_6$  starting material  $[\text{M} + \text{H}]^+$  ( $[m/z] = 4651.5$ ). Moreover, no shift in the low-energy UV/Vis absorption band I ( $\lambda_{\text{max}}$ ) at 592 nm was consistent with no change in Rh(II) coordination mode and there was no significant trace of Rh in the supernatant from ICP-OES analysis, confirming a clean and chemoselective alkene cleavage (Table S5, Figure S33).

## Conclusion

In summary, we have expanded our paradigm of Clip-off Chemistry to include a new step of retrosynthetic analysis. Unlike retrosynthesis in Organic Chemistry, which is based on the virtual dissection of bonds, retrosynthesis in Clip-off Chemistry entails virtually extending the product into a logical periodic material through cleavable bonds. As proof-of-concept, we employed our new retrosynthesis analysis in the Clip-off synthesis of four unprecedented, aldehyde-functionalised Rh(II)-based structures: a homoleptic cluster; a *cis*-disubstituted cluster; a macrocycle; and a crown-like architecture. Specifically, we used retrosynthesis to define the Rh-based MOP precursors functionalised with cleavable alkene bonds that would be required for the subsequent Clip-off synthesis of each target in high yield. We extensively characterised all four products. Considering this new retrosynthetic approach, and the fact that bond-breaking can be applied both selectively and quantitatively to precursors of different dimensionalities (from 3D to 0D), we anticipate that Clip-off Chemistry will complement existing synthetic methodologies to ultimately inform the design and synthesis of new molecules and materials.

## Acknowledgements

We thank Alba Cortés for her help with MALDI-MS measurements. This work has received funding from the European Union's Horizon 2020 research and innovation program under grant agreement No 101019003; the Grant Ref. PID2021-124804NB-I00 funded by MCIN/AEI/



10.13039/501100011033/ and by “ERDF A way of making Europe”; and the Catalan AGAUR (project 2017 SGR 238). It was also funded by the CERCA Programme/Generalitat de Catalunya. ICN2 is supported by the Severo Ochoa Centres of Excellence programme, Grant CEX2021-001214-S, funded by MCIN/AEI/10.13039/501100011033. F.G. acknowledges funding from the Spanish Research Agency (PID2021-123287OB-I00). Y.Y. acknowledges the China Scholarship Council for scholarship support.

### Conflict of Interest

The authors declare no conflict of interest.

### Data Availability Statement

The data that support the findings of this study are available from the corresponding author upon reasonable request.

**Keywords:** Bond Breaking · Clip-off Chemistry · Disassembly · Metal-Organic Polyhedra · Retrosynthetic Analysis

- [1] O. M. Yaghi, M. O’Keeffe, N. W. Ockwig, H. K. Chae, M. Eddaoudi, J. Kim, *Nature* **2003**, 423, 705–714.
- [2] S. Zhang, *Biotechnol. Adv.* **2002**, 20, 321–339.
- [3] J. E. Moses, A. D. Moorhouse, *Chem. Soc. Rev.* **2007**, 36, 1249–1262.
- [4] N. G. Schmidt, E. Eger, W. Kroutil, *ACS Catal.* **2016**, 6, 4286–4311.
- [5] K. G. Maskill, J. P. Knowles, L. D. Elliott, R. W. Alder, K. I. Booker-Milburn, *Angew. Chem. Int. Ed.* **2013**, 52, 1499–1502.
- [6] I. Alfonso, *Chem. Commun.* **2016**, 52, 239–250.
- [7] M. Hutin, D. Schultz, J. R. Nitschke, *Chimia* **2008**, 62, 198–203.
- [8] P. Shieh, M. R. Hill, W. Zhang, S. L. Kristufek, J. A. Johnson, *Chem. Rev.* **2021**, 121, 7059–7121.
- [9] L. Feng, S. Yuan, L. L. Zhang, K. Tan, J. L. Li, A. Kirchon, L. M. Liu, P. Zhang, Y. Han, Y. J. Chabal, H. C. Zhou, *J. Am. Chem. Soc.* **2018**, 140, 2363–2372.
- [10] Y. Yang, A. Broto-Ribas, B. Ortín-Rubio, I. Imaz, F. Gándara, A. Carné-Sánchez, V. Guillerme, S. Jurado, F. Busqué, J. Juanhuix, D. Maspoch, *Angew. Chem. Int. Ed.* **2022**, 61, e202111228.
- [11] H. C. Zhou, J. R. Long, O. M. Yaghi, *Chem. Rev.* **2012**, 112, 673–674.
- [12] M. Eddaoudi, J. Kim, J. B. Wachter, H. K. Chae, M. O’Keeffe, O. M. Yaghi, *J. Am. Chem. Soc.* **2001**, 123, 4368–4369.
- [13] S. Lee, H. Jeong, D. Nam, M. S. Lah, W. Choe, *Chem. Soc. Rev.* **2021**, 50, 528–555.
- [14] H. Furukawa, U. Müller, O. M. Yaghi, *Angew. Chem. Int. Ed.* **2015**, 54, 3417–3430.
- [15] J. Cho, Y. Ishida, *Adv. Mater.* **2017**, 29, 1605974.
- [16] H. Li, M. Eddaoudi, T. L. Groy, O. M. Yaghi, *J. Am. Chem. Soc.* **1998**, 120, 8571–8572.
- [17] X. Zhang, Z. Chen, X. Liu, S. L. Hanna, X. Wang, R. Taheri-Ledari, A. Maleki, P. Li, O. K. Farha, *Chem. Soc. Rev.* **2020**, 49, 7406–7427.
- [18] A. J. Gosselin, C. A. Rowland, E. D. Bloch, *Chem. Rev.* **2020**, 120, 8987–9014.
- [19] T.-Y. Luo, S. Park, T.-H. Chen, Prerna, R. Patel, X. Li, J. I. Siepmann, S. Caratzoulas, Z. Xia, M. Tsapatsis, *Angew. Chem.* **2022**, 134, e202209034.
- [20] A. M. Bumstead, I. Pakamori, K. D. Richards, M. F. Thorne, S. S. Boyadjieva, C. Castillo-Blas, L. N. McHugh, A. F. Sapnik, D. S. Keeble, D. A. Keen, R. C. Evans, R. S. Forgan, T. D. Bennett, *Chem. Mater.* **2022**, 34, 2187–2196.
- [21] J. Albalad, H. Xu, F. Gándara, M. Haouas, C. Martineau-Corcós, R. Mas-Ballesté, S. A. Barnett, J. Juanhuix, I. Imaz, D. Maspoch, *J. Am. Chem. Soc.* **2018**, 140, 2028–2031.
- [22] V. Guillerme, H. Xu, J. Albalad, I. Imaz, D. Maspoch, *J. Am. Chem. Soc.* **2018**, 140, 15022–15030.
- [23] E. J. Corey, *Pure Appl. Chem.* **1967**, 14, 19–38.
- [24] R. O. M. A. de Souza, L. S. M. Miranda, U. T. Bornscheuer, *Chem. Eur. J.* **2017**, 23, 12040–12063.
- [25] S. V. McCowen, N. A. Doering, R. Sarpong, *Chem. Sci.* **2020**, 11, 7538–7552.
- [26] R. Criegee, *Angew. Chem. Int. Ed.* **1975**, 14, 745–752.
- [27] C. R. Groom, I. J. Bruno, M. P. Lightfoot, S. C. Ward, *Acta Crystallogr. Sect. B* **2016**, 72, 171–179.
- [28] X. Song, X. Liu, M. Oh, M. S. Lah, *Dalton Trans.* **2010**, 39, 6178–6180.
- [29] M. J. Prakash, Y. Zou, S. Hong, M. Park, M. P. N. Bui, G. H. Seong, M. S. Lah, *Inorg. Chem.* **2009**, 48, 1281–1283.
- [30] J. Park, Y. P. Chen, Z. Perry, J. R. Li, H. C. Zhou, *J. Am. Chem. Soc.* **2014**, 136, 16895–16901.
- [31] L. Chen, T. Yang, H. Cui, T. Cai, L. Zhang, C. Y. Su, *J. Mater. Chem. A* **2015**, 3, 20201–20209.
- [32] B. Ortín-Rubio, H. Ghasempour, V. Guillerme, A. Morsali, J. Juanhuix, I. Imaz, D. Maspoch, *J. Am. Chem. Soc.* **2020**, 142, 9135–9140.
- [33] E. V. Dikarev, B. Li, H. Zhang, *J. Am. Chem. Soc.* **2006**, 128, 2814–2815.
- [34] Y. Lou, T. P. Remarchuk, E. J. Corey, *J. Am. Chem. Soc.* **2005**, 127, 14223–14230.
- [35] M. Ebihara, M. Nomura, S. Sakai, T. Kawamura, *Inorg. Chim. Acta* **2007**, 360, 2345–2352.
- [36] F. A. Cotton, J. L. Thompson, *Inorg. Chim. Acta* **1984**, 81, 193–203.
- [37] S. Sudan, R.-J. Li, S. M. Jansze, A. Platzek, R. Rudolf, G. H. Clever, F. Fadaei-Tirani, R. Scopelliti, K. Severin, *J. Am. Chem. Soc.* **2021**, 143, 1773–1778.
- [38] J.-R. Li, H.-C. Zhou, *Nat. Chem.* **2010**, 2, 893–898.
- [39] A. Broto-Ribas, M. S. Gutiérrez, I. Imaz, A. Carné-Sánchez, F. Gándara, J. Juanhuix, D. Maspoch, *Chem. Commun.* **2022**, 58, 10480–10483.
- [40] Deposition numbers 2281386 (for [Rh<sub>2</sub>(L<sub>1C</sub>)<sub>2</sub>]<sub>2</sub>), 2281052 (for [Rh<sub>2</sub>(3FBA)<sub>4</sub>]), 2281054 (for [Rh<sub>2</sub>(3FBA)<sub>2</sub>(4FBA)<sub>2</sub>]), and 2281053 (for [Rh<sub>2</sub>(3FBA)<sub>2</sub>(NDC)]<sub>6</sub>) contain the supplementary crystallographic data for this paper. These data are provided free of charge by the joint Cambridge Crystallographic Data Centre and Fachinformationszentrum Karlsruhe Access Structures service.

Manuscript received: July 20, 2023

Accepted manuscript online: September 6, 2023

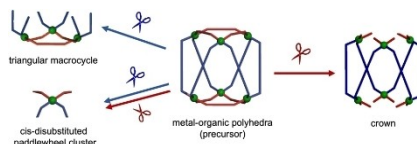
Version of record online: ■■■■■

## Research Articles

## Synthetic Coordination Chemistry

A. Broto-Ribas, S. Ruiz-Relaño, J. Albalad,\*  
Y. Yang, F. Gándara, J. Juanhuix, I. Imaz,\*  
D. Maspoch\* **e202310354**

Retrosynthetic Analysis Applied to Clip-off  
Chemistry: Synthesis of Four Rh(II)-Based  
Complexes as Proof-of-Concept



In Clip-off Chemistry, a retrosynthetic analysis step based on virtual extension of the products through cleavable bonds enables defining the required precursor materials. As proof-of-concept, this new approach is used to synthesize four aldehyde-functionalised Rh(II)-based complexes: a homoleptic cluster; a *cis*-disubstituted paddlewheel cluster; a macrocycle; and a crown.